SENSITIVITY ANALYSIS OF THE SNGR METHOD APPLIED TO JET NOISE

M. Mesbah, J. Meyers, W. Desmet, M. Baelmans
Department of Mechanical Engineering , K.U.Leuven
Celestijnenlaan 300A, 3001 Leuven, Belgium
majid.mesbah@mech.kuleuven.ac.be

ABSTRACT

A hybrid three-step approach is applied to simulate the flow noise generated by a high-speed subsonic round jet with $D = 25$ mm and $M = 0.86$. The computations are performed in a 2D-axisymmetric co-ordinate system. An average flow solution obtained from RANS is used to construct a stochastic turbulent velocity field. The acoustic source terms resulting from this fluctuating velocity field are subsequently used for the computation of the acoustic intensity in the far field by solving the axisymmetric linearized Euler equations. All simulation results are compared with the experiments of Lush (J. Fluid Mech., 1971 Vol. 46, pp.477–500). Further, the repeatability of the method is evaluated and the effect of some important parameters to the SNGR such as the number of modes, the spectral energy profile and the wave number sampling on sound intensity are investigated.

INTRODUCTION

In recent years a lot of effort has been spent on the simulation of aero-acoustic noise. This aero-acoustic noise can be categorized into broadband noise and tonal noise. Tailor-made simulation methods exist for both these noise categories. Several prediction methods have been proposed for broadband flow induced noise. In the present paper an engineering method for predicting broadband noise is presented as will be discussed in more detail. The paper concentrates on the study of jet noise, which is a representative example of flow-generated broadband noise.

In the Stochastic Noise Generation and Radiation (SNGR) method, originally presented by Karweit (1991) and Bechara *et. al.* (1994), a random velocity field is generated by a finite sum of discrete Fourier modes based upon averaged data of the flow field. In a further development, Bailly *et. al.* (1995) add a time dependent term in these Fourier modes. Billson *et. al.* (2003) solve a convection equation for the time filtered turbulent velocity field in each time step in order to include convection effects. In the SNGR method, the generated random velocity field is used to determine the aero-acoustic sources for acoustic perturbation. Thereby, the Euler equations, which are linearized around a mean flow, are considered as an appropriate wave operator. Furthermore, it is assumed that the turbulent field is not influenced by the acoustic waves. To summarize, calculations associated with SNGR methods may be discerned in three steps:

1. A Reynolds-Averaged Navier-Stokes solution (RANS), e.g., closed with a k–ϵ turbulence model, provides time-averaged information of the flow field.

2. An isotropic turbulent velocity field based on random Fourier modes is generated using the data obtained from the previous step.

3. In the last step the Linearized Euler Equations (LEE), with unsteady source terms induced by the fluctuating velocity field, are solved.

The SNGR method provides a low computational cost for CAA simulations. However, this method overpredicts the acoustic sound intensity when it is applied to a free jet. Furthermore, the reconstruction of the turbulent velocity field which has a significant effect on the far field noise, is a crucial step in the SNGR method. Therefore, the aim of this work is to assess the sensitivity of the far field noise to different parameters used to generate the turbulence field.

The paper is organized as follows. First, a method to generate a turbulent velocity field is introduced. Next, the two-dimensional axisymmetric LEE is discussed to gather with its numerical implementation. The numerical scheme and boundary conditions employed to solve the two-dimensional axisymmetric LEE are described. Subsequently, the set-up and results of the reference simulation obtained from RANS are discussed. The effect of different parameters on the far-field noise results are further elaborated in the successive section. Finally, conclusions are summarized in the last section.

STOCHASTIC TURBULENCE MODELLING

A method to simulate a space-time stochastic turbulent velocity field has been developed by Bailly *et. al.*(1995). To this end, an isotropic turbulent field is constructed as a finite sum of discrete Fourier modes, i.e.,

$$\mathbf{U}_t(\mathbf{x},t) = 2\sum_{n=1}^{N} \widetilde{u}_n \cos[\mathbf{k}_n.(\mathbf{x} - t\mathbf{U}_c) + \psi_n + \omega_n t]\boldsymbol{\sigma}_n. \quad (1)$$

where $\widetilde{u}_n$, ψ_n, and $\boldsymbol{\sigma}_n$ are the amplitude, phase, and direction of the n^{th} Fourier mode, respectively. Moreover, $\mathbf{U}_c$ is the local convection velocity and ω_n is the angular frequency of the n^{th} mode. The angular frequency ω_n is randomly selected with a Gaussian probability density function, i.e.,

$$P(\omega_n) = \frac{1}{\omega_{0n}\sqrt{2\pi}}\ \exp[-\frac{(\omega-\omega_{0n})^2}{2\omega_{0n}^2}],\ \text{with}\ \omega_{0n} = u^{'}k_n\ . \quad (2)$$

where the wave number $k_n = \| \mathbf{k}_n \|$. Further, $u^{'} \simeq (2\overline{k}/3)^{1/2}$ is the estimated turbulent velocity, which is obtained from RANS. The wave vector $\mathbf{k}_n$ is chosen randomly on a sphere with radius k_n. Figure 1 shows a sketch of the geometry. Assuming incompressibility of the turbulent velocity field,

$\mathbf{k}_n.\boldsymbol{\sigma}_n = 0$ for all modes in frequency space.The probability density functions used to generate the random distributions for $\mathbf{k}_n$ and $\boldsymbol{\sigma}_n$ are presented in Table 1.

Table 1: Probability density functions

$P(\varphi_n) = 1/(2\pi)$	$0 \leq \varphi_n \leq 2\pi$
$P(\psi_n) = 1/(2\pi)$	$0 \leq \psi_n \leq 2\pi$
$P(\alpha_n) = 1/(2\pi)$	$0 \leq \alpha_n \leq 2\pi$
$P(\theta_n) = (1/2)\sin(\theta)$	$0 \leq \theta_n \leq \pi$

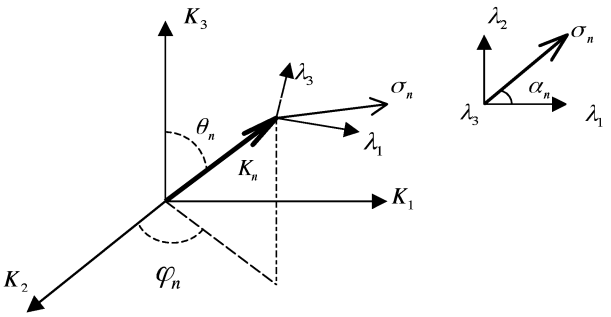

Figure 1: Schematic of the wave vector $\mathbf{k}_n$ and the perpendicular vector of $\boldsymbol{\sigma_n}$

The Von Karman-Pao spectrum is employed to simulate the energy spectrum for isotropic turbulence

$$E(k) = A\frac{2\overline{k}}{3k_e}\frac{(k/k_e)^4}{[1+(k/k_e)^2]^{17/6}}\exp(-2\frac{k}{k_\eta}), \tag{3}$$

where $k_\eta = \varepsilon^{1/4}\nu^{-3/4}$ is the Kolmogorov wave number. The parameters A and k_e determine the shape of the spectrum and the distribution of energy over different wave numbers. The integral of the energy spectrum over all wave numbers should be equal to the total turbulent kinetic energy.

$$\overline{k} = \int_0^\infty E(k)\ \mathrm{d}k \tag{4}$$

The numerical constant A can be obtained from Equation (4) combined with an infinite-Reynolds-number assumption, leading to $A = 1.453$. The parameter k_e, is calculated assuming that the turbulent length scale equals the integral length scale L

$$k_e = \frac{9\pi}{55}\frac{A}{L}. \tag{5}$$

where

$$L = f_L\frac{u'^3}{\varepsilon}, \tag{6}$$

the parameter f_L is a factor of order unity, introduced here for the sake of later convenience.

The spectrum $E(k_n)$ is discretized into N points with a minimum wave number k_1 and maximum wave number k_N. In this paper both linear distribution and logarithmic distribution are used. The selection of k_1 and k_N will be further discussed later. The amplitude $\widetilde{u}_n$ of each discrete mode is related to the energy spectrum $E(k_n)$, i.e.,

$$\widetilde{u}_n = \sqrt{E(k_n)\Delta k}, \tag{7}$$

where Δk is the spacing of the wave number distributions. Further, it is clear that

$$\overline{k} = \sum_{n=1}^{N}\widetilde{u}_n^2. \tag{8}$$

LEE SOLVER

The SNGR method relies on the fact that linearized Euler equations are considered as an appropriate wave operator for acoustic perturbations. Typically, different methods are presented in the literature to linearize the Euler equations (Bachara, 1994, Bailly, 1995, Billson, 2002), leading to different source terms. In this research, LEE with the source terms described by Bailly (1995), are employed as wave operator. These equations in 2-dimensional axisymmetric co-ordinates and written in conservative form are used in this research (Mesbah et.al., 2004). The last step of the SNGR method, is solving LEE. Hence, a code is written to solve the LEE for axisymmetric case. All spatial derivatives are discretized by a seven-point finite difference scheme, corresponding to the Dispersion-Relation-Preserving (DRP) scheme of Tam *et. al.*(1993). The artificial selective damping is employed to eliminate spurious numerical oscillations (Tam, 1995). For the time integration, the second-order five-stages Low-Dispersion-Dissipation Rung-Kutta scheme of Bogey *et. al.*(2004) is used. The outflow and radiation boundary conditions of Tam (1997) are implemented at the boundaries. In order to correspond to the axisymmetric LEE, these boundary conditions are slightly altered here (Mesbah *et. al.*, 2004).

SET-UP AND RESULTS OF THE REFERENCE SIMULATION

A high-speed subsonic jet with Mach number $M = 0.86$, and nozzle diameter $D = 25$ mm , is simulated using the above described SNGR method. This setup corresponds to the experiment presented by Lush (1971), which was used before as a point of reference for SNGR validation (Bailly, 1994,1995). In the following subsections some aerodynamic and acoustic results will be discussed.

Flow Results

The mean flow solution is obtained from a RANS simulation, using a k–ϵ model. This simulation is performed using the CFX4.3 solver.[1] The computations are performed for the axisymmetric case on a domain with size $5D \times 20D$. Figures 2 (a) and (b) show the mean velocity $\overline{U}$ in the jet direction and the turbulent kinetic energy, respectively. The presented results do well agree with results in the literature (Bailly, 1994).

Acoustic Results

As already mentioned in the first section, the aim of this research is the assessment of different parameters in SNGR

[1] CFX International, AEA Technology, Harwell, Didcot, Oxon., UK,1997

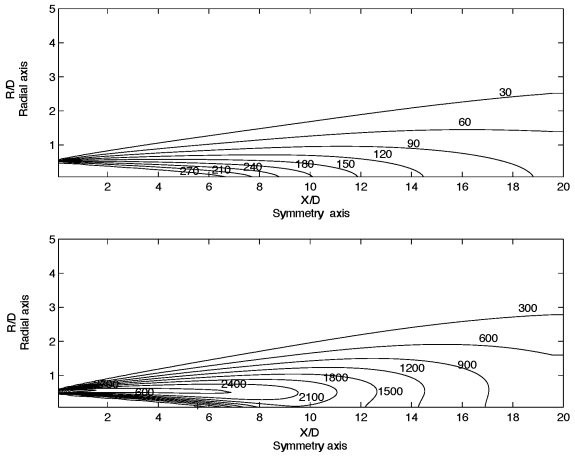

Figure 2: (a) U-velocity component ($\frac{\mathrm{m}}{\mathrm{s}}$) , (b) Turbulent kinetic energy ($\frac{\mathrm{m}^2}{\mathrm{s}^2}$)

methods. Therefore, first a reference simulation is performed using the same set–up as presented by Bailly (1995, 1999). In these references the source region is limited to points where the turbulent kinetic energy $\overline{k} > 0.3\overline{k}_{max}$. The lower and upper wave number are $k_1 = k_{emin}/5$ and $k_N = 2\pi/7\Delta x$, respectively, with k_{emin} the smallest value of k_e over the source volume. The wave number range is discretized using $N = 30$ modes. Figure 3 shows the sketch of the acoustic computational domain. The calculations are performed on an axisymmetric domain which extends $20D \times 20D$. The mesh has a constant mesh size $\Delta x = \Delta r = 1.53 \times 10^{-3}$ m. The time step $\Delta t = 1.2 \times 10^{-6}$ seconds, corresponding to a CFL number of 0.5. The computation covers a time interval $T = 3.84 \times 10^{-3}$ seconds, which corresponds to 3,200 time steps. The analysis is performed over the last 1,500 time steps of the computation. The acoustic signals are recorded at locations $R_c = 19.5D$ (centered at the jet exit) and $\theta = 15°, 20°, ..., 90°$ (see Figure 3).

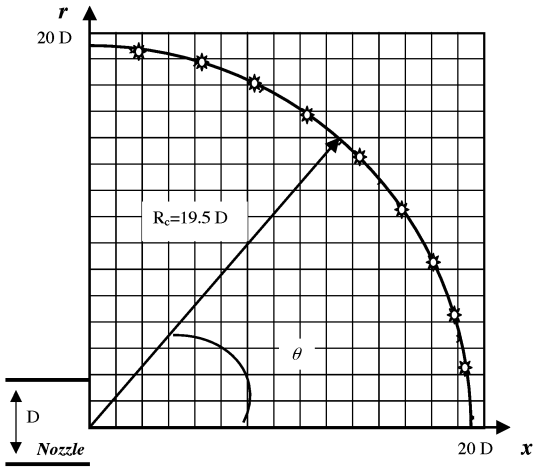

Figure 3: Sketch of the acoustic computational domain

For reference, the acoustic intensity L_I, is defined as

$$L_I = 10\log(\frac{I}{I_{ref}}) \qquad \text{(dB)}, \tag{9}$$

where $I_{ref} = 10^{-12}$ ($\frac{\mathrm{W}}{\mathrm{m}^2}$) and

$$I = \overline{P_a \cdot \sqrt{U_a^2 + V_a^2}} \qquad (\frac{\mathrm{W}}{\mathrm{m}^2}) \ . \tag{10}$$

In case the recorded signal is situated in the far-field, equation (10) can be approximated by

$$I \approx \frac{\overline{P_a^2}}{\overline{\rho} c} \qquad (\frac{\mathrm{W}}{\mathrm{m}^2}) \ . \tag{11}$$

In order to compare the results with Lush's experimental data (Lush, 1971), the measured acoustic intensity in equations (10) and (11) is scaled with $(120D/19.5D)^2$. As can be appreciated from Figure 4, the simulation overpredicts the measurement with approximately 7 dB. Similar studies using the SNGR methodology likewise show overpredictions of the generated far field sound, roughly corresponding to 10% of the experimental sound level (Bailly, 1995, Billson, 2003).

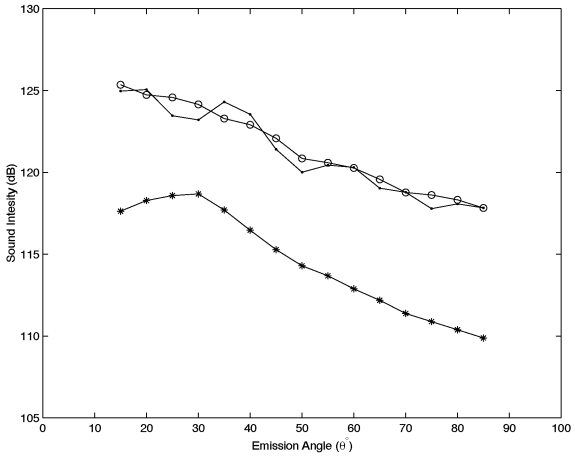

Figure 4: Sound intensity at different angles θ. The simulations are performed with $N = 30$, $k_1 = \frac{k_{emin}}{5}$, $k_N = \frac{2\pi}{7\Delta x}$, $f_L = 1$, Source region $\frac{\overline{k}}{\overline{k}_{max}} > 0.3$. (–):Reference simulation. (–o–):Sound intensity averaged over 20 SNGR simulations. (–*–):measurement.

ASSESSMENT OF DIFFERENT PARAMETERS IN THE SOURCE-GENERATING ALGORITHM

The effect of some parameters such as the energy spectrum and the extent of the source region on the far field sound were investigated in an earlier study (Mesbah *et. al.*, 2004). It was shown that a variation of the random-number series causes a scatter in results. Furthermore, the results indicated that the sensitivity analysis should be extended to more parameters in order to define the effect of each parameter on the far field noise precisely. In the present paper the following parameters and properties are investigated:

- the repeatability of the method,
- the number of modes N by which the spectral energy profile is discretized,
- the spectral energy profile,
- the wave number sampling.

Repeatability of the method

The effects on sound intensity due to a variation of random number series is investigated by using 20 simulations. Figure (4) shows the sound intensity at different angles θ and the average over twenty different random SNGR realizations. It can be seen that the average is clearly much smoother than the individual SNGR results. As such, a trade off between computational cost and accuracy exists. Figure 5 presents the absolute value of the deviation from the mean value at each observation point for different number of simulations. The deviation is estimated by using the Student distribution with a confidence interval of 95%. It can be seen that the sound intensity at $\theta = 40$, 60 and 80°, has the lowest deviation (≈ 0.4 dB) from the mean value and is not influenced by averaging over more simulations. Further, a reduction in deviation with approximately 0.5 dB, is observed when the number of simulations used for averaging increases from 4 to 20.

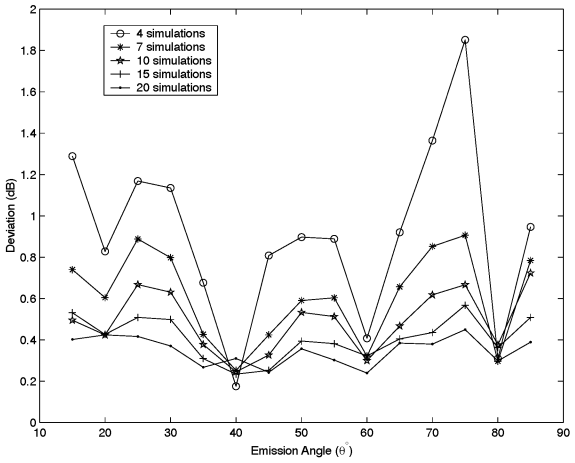

Figure 5: Deviation from mean intensity value

Number of modes N

It is important to quantify how many modes should be included before N-independent results are obtained. In order to quantify this, simulations are performed for 30, 90, 180 and 360 modes. The effect of N on the far-field sound intensity for the average over 20 simulations is presented in Figure 6. It is observed that the sound intensity increases when the number of modes N increases from 30 to 90. The increase varies from 2 dB at $\theta = 15°$ to 1 dB at $\theta = 85°$. Furthermore, by increasing N from 90 to 360, the sound intensity decreases so that the obtained results for $N = 360$ is similar to the results for $N = 30$. However, the gap with experimental results remains 7 dB. It is not expected to drastically lower this gap by increasing the amount of modes.

Spectral energy profile

The effect of the energy spectrum on the far field noise is studied by Billson (2003) and Mesbah (2004). It is observed that increasing the length scale factor f_L (see equation (6)) from 1 to 6, results is a decrease of the acoustic sound intensity. In order to investigate these trends more rigourously, variations of the amplitude of each mode are displayed for a typical source point in Figure (7). It can be seen that k_e

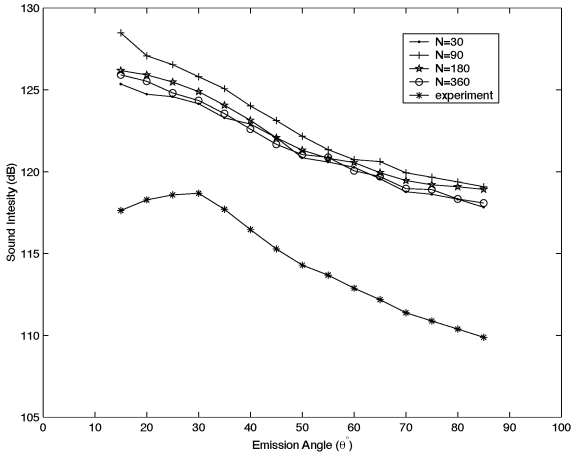

Figure 6: Average of sound intensity for different mode number

(the wave number in which the spectrum has a maximum value) decreases and that the shape of spectrum becomes sharper for increasing values of f_L. Note that for $f_L = 6$ and $\theta < 30°$, far-field assumption is only approximately valid and small differences exist between the sound intensity evaluation according to equations (10) and (11). In principle, this difference can be removed by using a larger simulations domain. However, in order to correctly capture the sound intensity, equation (11) is used to evaluate the results. Figure (8) shows the results for $f_L = 6$ and $N = 30$, 90, 180, 360. The presented results are obtained by averaging over 4 simulations for each number of modes. As can be seen, similar to the results presented in Figure (6) for $f_L = 1$, increasing the number of modes has a nonlinear effect on the acoustic sound intensity. The difference between $N = 30$ and $N = 90$ roughly amounts to 4 dB. Further, increasing N from 90 to 360, decreases this difference to 1 dB. Table 1 presents the summation of the calculated kinetic energy of all wave numbers for different modes and different spectral profiles. The data is normalized with the total energy integrated over the entire selected source region. The results show that the higher the change in energy contents, the higher the change in sound intensity is for different number of modes. However, the trend of increasing energy content with increasing number of modes (for $f_L = 6$) does not necessarily result in an increase of sound intensity. As such it can be concluded that there is a non-linear relation between energy contents and sound intensity. Furthermore, it should be noticed that when the spectrum has a pronounced maximum , i.e. $f_L = 6$, more modes should be employed to calculate the energy accurately. As such one can conclude that in this case also the sound intensity is much more sensitive to changes in number of modes

Table 2: Percentage of the calculated energy. The wave number has a linear sampling

N	30	90	180	360
$f_L = 1$	100.32	100.10	100.05	100.02
$f_L = 6$	70.29	96.80	100.04	100.02

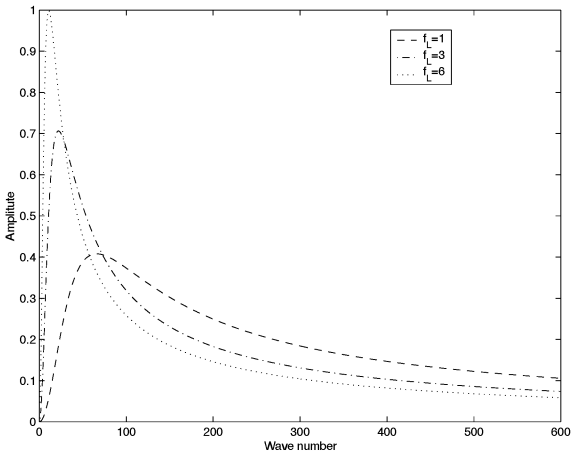

Figure 7: Spectral energy profile

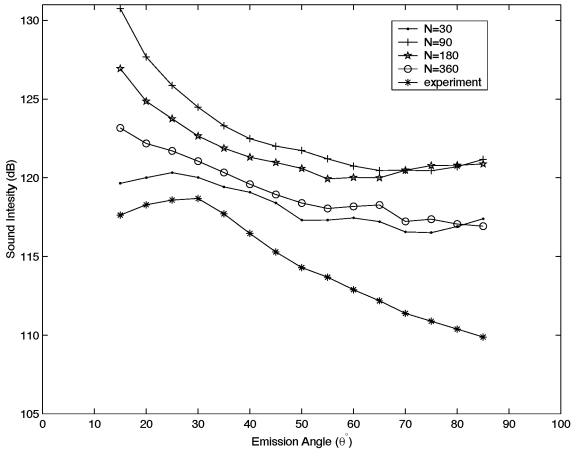

Figure 8: Sound intensity at different angles θ. $f_L = 6$

The wave number sampling

For the implementation of the SNGR method, a linear or logarithmic sampling of the wave number can be employed. When a logarithmic sampling is used, the amplitude of the modes at the low wave numbers are suppressed while the amplitudes of modes at the high wave numbers are amplified due to the increasing Δk_n in equation (7) for higher wave numbers (Billson, 2003). However, the logarithmic wave number sampling can calculate the energy with reasonable accuracy when the spectrum has a pronounced maximum. In this section simulations for $f_L = 1$ and $f_L = 6$ are performed using a logarithmic sampling and compared to simulation with a linear wave number discretization. Table 2 presents the percentage of calculated kinetic energy of all wave numbers for different modes and different spectral profiles. It is seen that for $f_L = 1$, the linear discretization results in a more accurate energy computation than the logarithmic one. In contrast, with the logarithmic discretization the energy for $f_L = 6$ is more precisely estimated compared to the linear discretization, especially when a low mode number is employed.

Estimated acoustic intensity for $f_L = 1$ and $f_L = 6$ are presented in Figure (9) and (10), respectively. A comparison between Figure (9) and (6) for $f_L = 1$ indicates less variation in sound intensity due to variation in N, compared to the simulation when a linear sampling is used. Furthermore, the obtained results for $N = 360$ for both samplings are almost identical whereas the difference in results for $N = 90$ amounts to 5 dB. Results exhibit a non-monotonous variation when the number of modes increases. The results from this section and previous sections reveal that both the wave number sampling and the contained energy of each mode have a significant effect on this non-monotonous behavior. In order to further investigate this behavior, more simulations for different number of modes should be performed.

Table 3: Percentage of the calculated kinetic energy by Logarithmic sampling wave number

N	30	90	180	360
$f_l = 1$	102.17	100.59	100.28	100.13
$f_l = 6$	101.56	100.29	100.12	100.05

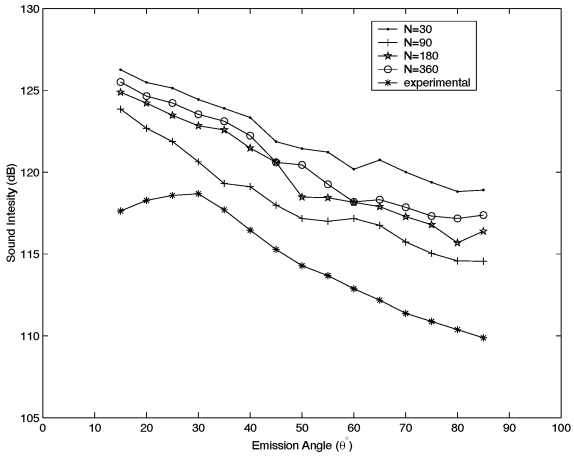

Figure 9: Logarithmic sampling of wave number for $f_L = 1$

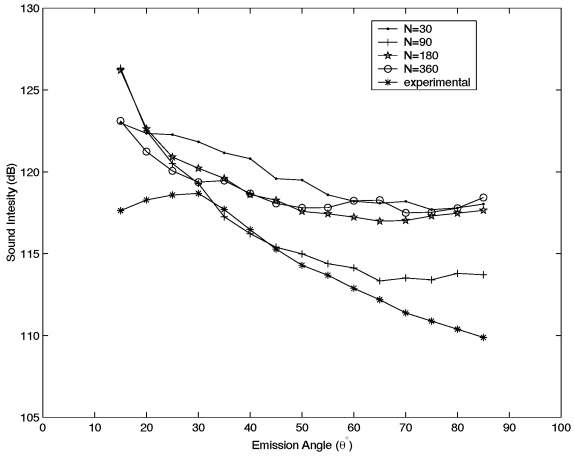

Figure 10: Logarithmic sampling of wave number for $f_L = 6$

CONCLUSIONS AND FUTURE STEPS

An application of an engineering method which combines stochastic turbulent field with computational fluid dynamic to a near sonic two dimensional axisymmetric jet is presented. A RANS solution provides the time-averaged mean flow field. Based on this mean flow solution, a stochastic turbulent velocity field is generated. This turbulent field is then used to generate the source for a LEE solver. The solution of this LEE system eventually provides the far-field broadband noise. Further, acoustic intensities in the far field are computed by solving the LEE numerically.

In the present study, the SNGR setting selected by Bailly *et. al.*(1999) is considered as a reference. This reference simulation overestimates the acoustic intensity roughly by 7 dB. A sensitivity analysis was performed on the effect of some SNGR parameters (Mesbah *et. al.*, 2004) in order to investigate this inconsistency. In the present paper, this study is further extended and the effect of properties such as repeatability of the method, number of modes, spectral energy profile and wave number sampling on the sound intensity are investigated. Several conclusions can be summarized. The repeatability of the method can be improved by averaging over various simulations. Moreover, the deviations from mean value are presented for averaging over different number of simulations that helps to trade off between computational cost and accuracy. The results show that increasing the number of modes has a non-monotonous effect on acoustic intensity. The calculated energy for different spectral-energy shapes indicates that high number of modes should be employed in order to calculate the energy accurately when the spectrum has a pronounced maximum. Analysis of the wave number sampling and the variations in spectral-energy shape by increasing the integral length scale factor f_L reveals that energy of higher wave numbers has a significant effect on the acoustic intensity. In order to further investigate this non-linear behavior more simulations for more wave numbers should be performed. This is the subject of future research.

REFERENCES

Karweit, M., Belanc-Benon, P., Juve, D., Comte-Billot, G., 1991, "Simulation of the propagation of an acoustic wave through a turbulent velocity field: A study of phase variance", Journal of Acoust. Soc. Am. 89(1), pp. 52-62.

Bechara, W., Bailly, C., Lafon, P. , 1994, "Stochastic Approach to Noise Modeling for Free Turbulent Flows", Journal of Acoust. Soc. Am. 97(6), pp. 3518-3531.

Bailly,C., Lafon, P., Candel, S., 1995, "A Stochastic Approach to Compute Noise Generation and Radiation of Free Turbulent Flows", AIAA Paper, 95-092-1-6.

Bailly,C., Juve, D., 1999, "A Stochastic Approach To Compute Subsonic Noise Using Linearized Euler's Equations", AIAA paper 99-1872.

Billson, M., Eriksson, L. E., Davidson, L., 2002, "Acoustic Source Terms for the Linear Euler Equations on Conservative Form", AIAA paper, No.2582, Breckenridge.

Billson, M., Eriksson, L. E., Davidson, L., 2003, "Jet Noise Prediction Using Stochastic Turbulence Modeling", AIAA paper, No. 3282, 9th AIAA/CEAS Aeroacoustics Conference, Hilton Head.

Mesbah, M., Meyers, J., Baelmans, M., Desmet, W.,2004, "Assessment of different parameters used in the SNGR method, Proceedings of the International Conference on Noise and Vibration, pp. 389-402, ISMA2004, September 21-23, Leuven.

Tam, C.K.W., 1998, "Advances in Numerical Boundary Condition for Computational Aeracoustics", Journal of Computational Acoustics, vol. 6, 377-402.

Tam, C.K.W., "Computational Aeroacoustics: Issues and Methods", AIAA Journal, 33(10), 1788-1796.

Tam, C. K.W., Webb, J. C., 1993 "Dispersion-Relation-Preserving Finit Difference Scheme for Computatianal Acoustics", Jornal of Computational Physiscs, (107), pp. 262-281.

Bogey, C., Bailly, c., 2004, "A Family of Low Dispersive and Dissipative Explicit Scheme for Flow and Noise Computations", Journal of Computational Physics, (194), pp. 194-214.

Bailly, C., Lafon, L., Candel, S., "Computation of Subsonic and Supersonic Jet Mixing Noise Using a Modified $\kappa-\epsilon$ Model for Compressible Free Shear Flows", Acta Acoustica, Vol. 2, pp. 101-112.

Lush, P.A., 1971, "Measurements of Subsonic Jet Noise and Comparison with Theory", Journal of Fluid Mechanics, Vol. 46, pp.477-500.